Journal of Alloys and Compounds 527 (2012) 117–121

Contents lists available at SciVerse ScienceDirect

Journal of Alloys and Compounds

journal homepage: www.elsevier.com/locate/jallcom

Microstructural investigation of in situ TiB whiskers array reinforced ZrB_2–SiC joint

Weiqi Yang[a], Tiesong Lin[a], Peng He[a,*], Yudong Huang[b], Jicai Feng[a]

[a] State Key Laboratory of Advanced Welding and Joining, Harbin Institute of Technology, Harbin 150001, China
[b] School of Chemical Engineering and Technology, Harbin Institute of Technology, Harbin 150001, China

ARTICLE INFO

Article history:
Received 16 December 2011
Received in revised form 27 February 2012
Accepted 4 March 2012
Available online xxx

Keywords:
Ceramics
Transition metal alloys and compounds
Microstructure
Mechanical properties

ABSTRACT

The ZrB_2–20 vol.% SiC composites (ZS) were joined to themselves using an Ag–Cu/Ti filler alloy. A novel TiB whiskers (TiBw) array with high preferred orientation was in situ synthesized at the interface of ZS. Investigation showed that the produced $AgCu_4Zr$ together with sufficient Ti promoted dissolution of ZrB_2, and subsequently led to the formation of TiBw array. The mechanical properties of ZS/ZS joint were improved by interfacial TiBw accommodation. The maximum shear strength of 146 MPa was obtained with the filler alloy containing 15 wt.% Ti.

1. Introduction

ZrB_2–SiC composites have attracted great attention due to their unique mechanical and physical advantages [1,2]. In particular, the lowest theoretical density among the ultra-high temperature ceramics (UHTCs) makes ZrB_2–SiC composites promising materials for application in aerospace fields [3–5]. However, like most ceramics, the fabrication of ZrB_2–SiC composites with large dimensions and complex shapes is difficult due to their brittle and hard properties. Therefore, the development of robust joining techniques capable of assembling smaller and geometrically simple parts is quite necessary [6].

For conventional brazing methods, one of the biggest challenges is the stresses induced by the mismatch in coefficient of thermal expansion (CTE) between the both heterogeneous materials that impair the joint integrity. In order to overcome this problem, some low CTE materials (such as SiC [7–9], Al_2O_3 [10], TiC [11]) have been incorporated in the brazing alloy. However, direct addition has its intrinsic limitations, such as inhomogeneous distribution, poor wettability, etc. [10]. Recent studies [12,13] demonstrate that in situ synthesized TiBw with advantages of fine size, relative stability and compatibility, can relieve residual stress and increase shear strength of joints to some extent. However, uncontrolled precipitation of TiBw during cooling process usually leads to aggregation and disordered orientation, which are unfavorable to the joint. Besides, the joint interface as the weakest region can't be effectively improved due to lack of reinforcements. If the TiBw can orderly distribute on the interface between ZS and filler alloy, it will be ideal to relax joint stress and increase joint strength. Unfortunately, up to now, there is no relevant report in the literature to the best of our knowledge.

In the present work, a novel TiBw array was in situ synthesized on the interface between ZS and filler alloy during brazing process. The typical interfacial microstructure of ZS was characterized and the formation mechanism of TiBw was analyzed. In addition, the effects of the Ti contents on the interfacial microstructure and shear strength of ZS/ZS brazing joints were also studied systematically.

2. Experimental procedures

The ZrB_2–20 vol.% SiC composite (ZS) was fabricated by hot pressing at 2000 °C/30 MPa for 1 h with starting materials ZrB_2 and SiC. The raw ZS was sliced into 6 mm × 6 mm × 3.5 mm pieces and 20 mm × 10 mm × 3.5 mm pieces for metallographic observation and strength test, respectively. The joining material for typical microstructural observation was Ag–Cu/Ti lamination, which was constructed by commercially available Ag–Cu (73Ag–27Cu (wt.%)) foil (100 μm in thickness) and pure Ti foil (40 μm in thickness). In order to investigate the effect of Ti content on the microstructure and mechanical properties of ZS/ZS joint, Ti powder with particle size of 300 mesh was added into Ag–Cu (73Ag–27Cu (wt.%)) filler alloy powder. Then the mixture was milled for 2 h in an argon atmosphere using a QM-SB planetary ball mill to prepare the new filler alloys with Ti content of 5%, 10%, 15% and 20% (wt.%), respectively.

Prior to joining, the brazing surface of ZS was polished by diamond grinding disc up to 800-grit. All the specimens were cleaned by ultrasound in acetone for 10 min and sequentially air-dried. The filler alloy was placed between the brazing couples. The assembly was put in a vacuum furnace with the vacuum of 3×10^{-4} MPa and heated to 750 °C at a rate of 15 °C min^{-1}, isothermally held for 5 min, and then

* Corresponding author. Tel.: +86 451 86402787; fax: +86 451 86402787.
E-mail address: hithepeng@hit.edu.cn (P. He).

0925-8388/$ – see front matter © 2012 Elsevier B.V. All rights reserved.
doi:10.1016/j.jallcom.2012.03.016

Table 1
Average chemical compositions of brazed joint by EDS (at.%).

Points	Elements (at.%)							Possible phase
	Ti	Cu	Ag	Zr	Si	B	C	
1	44.47	6.92	0.05	1.42	10.00	–	37.14	Ti_3SiC_2/TiCu
2	71.15	22.61	0.69	0.96	4.59	–	–	Ti_2Cu/Ti_5Si_3
3	3.14	67.75	14.67	14.17	0.27	–	–	$AgCu_4Zr$
4	44.69	51.30	2.22	1.51	0.28	–	–	TiCu
5	0.21	0.31	0.07	12.90	0.15	86.36	–	ZrB_2
6	0.64	10.00	87.82	0.60	0.94	–	–	Ag(s,s)

further heated to 900 °C at a rate of 10 °C min^{-1}, isothermally held for 10 min, and next cooled to 400 °C at a rate of 5 °C min^{-1}, finally, the furnace was cooled down spontaneously to room temperature.

Polished cross-sections of the brazing joints were characterized by scanning electron microscopy (SEM, S-4700) equipped with energy dispersive X-ray spectroscopy (EDS, TN-4700). Nanoindentation tests were carried out across the joint using a Nano-Indenter XP (Agilent Co.) with a Berkovich diamond indenter under a maximum load of 80 mN and loading time of 30 s. An average of at least six points was used to determine the hardness for each region in the joint. The shear strength of the joints at room temperature was examined using an Instron-1186 universal testing machine at a shear rate of 0.5 mm min^{-1}. For each set of experimental condition, at least six samples were used to average the joint strength. The uncertainties of data set in nanoindentation and shear strength tests were evaluated by standard deviation. The X-ray diffraction (XRD JDX-3530M) spectrometer with Cu-Kα radiation was employed to identify interfacial compounds by performing on fracture surface which cracked at the brazed seam after shear test.

3. Results and discussion

3.1. Typical microstructure of the ZS/ZS joints

Fig. 1 shows the cross-sections of ZS/ZS joint brazed with Ag–Cu/Ti lamination at 900 °C for 10 min. The general view in Fig. 1(a) confirms that the self-joining of the ZS with Ag–Cu/Ti interlayer was successfully achieved. On the ZS surface, two reaction layers with a width more than 10 μm respectively were formed, it is noteworthy that a grass-like phrase with high preferred orientation was found in layer I. Layer II consists of a gray and a dark gray phase appearing as strip-like, they distribute alternatively between layer I and the Ag-based solid solution (Ag(s,s)) at the center of the joint. Some blocks were found in Ag(s,s) due to excess Ti in filler alloy. From the magnified image of Ag(s,s) in Fig. 1(b), it was observed that some nano-particles scattered in the center of the joint. This compound is probably TiC, which was produced by a series of reactions between Ti–Cu liquid and SiC.

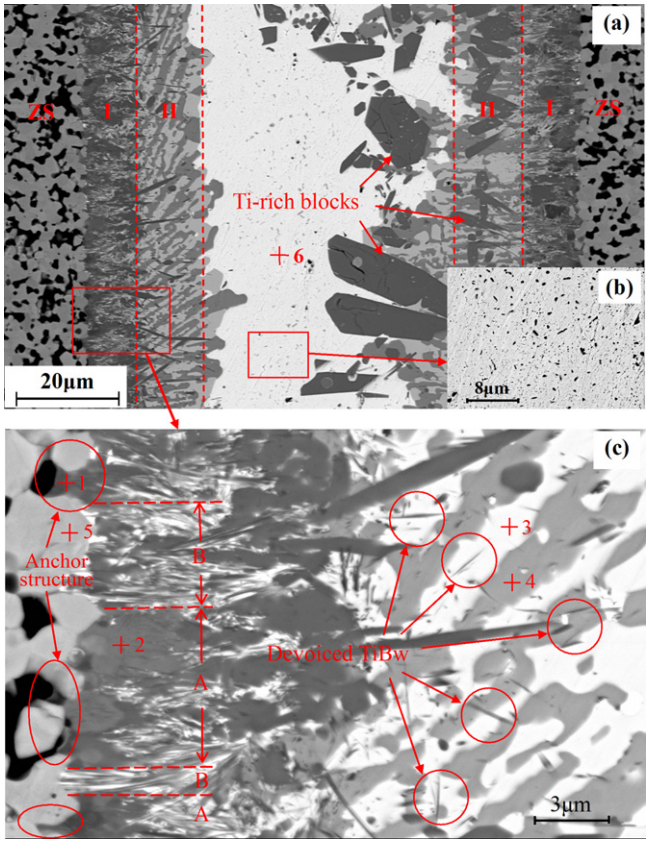

Fig. 1. Backscattered electron micrographs of ZS/ZS joint brazed by Ag–Cu/Ti lamination at 900 °C for 10 min: (a) microstructure of the joint; (b) and (c) magnifications of the marked areas in (a).

From the magnified image, in Fig. 1(c), it can be observed that the interfacial microstructure of ZS substrate is mainly composed of two parts: the SiC product area (section A) and the ZrB_2 product area (section B). During brazing process, SiC reacted with the liquid alloy violently, severe reaction led to the depletion of SiC distributed on the ZS surface. The compound produced by the reactions of SiC and filler alloy grew in the former SiC site to form "compound island". In some cases, as the surface SiC was exhausted, the liquid alloy could fill into the inside of ZS to form an "anchor structure" (as shown in Fig. 1(c)), which is beneficial to the joint strength. According to the analysis of EDS, as shown in Table 1, the dark phase (point 1), which is adjacent to SiC, appears in the form of Ti_3SiC_2. The "compound islands" (point 2) in section A mainly comprise of Ti_2Cu and Ti_5Si_3. In the ZrB_2 product area, no continuous compound layer was formed. The surface of ZrB_2 was contacted with a gray phase, where the grass-like TiBw grew vertically from the ZrB_2 surface to layer II. The lengths of TiBw range from hundreds of nanometers to more than 10 μm, some of them detached from base clusters and flowed to layer II. The XRD patterns (shown in Fig. 2) obtained from the fracture surface of brazing joints confirm that the phases of the seam contained TiB, Ti_2Cu and Ag. The EDS

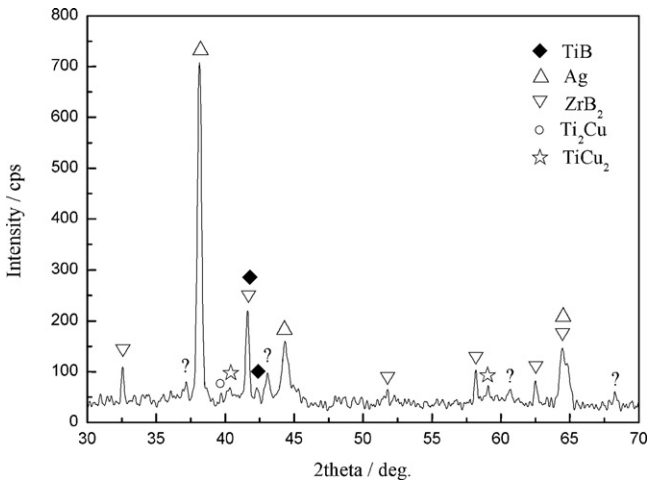

Fig. 2. XRD pattern of the fracture surface after shear test for specimens brazed with Ag–Cu/Ti lamination at 900 °C for 10 min.

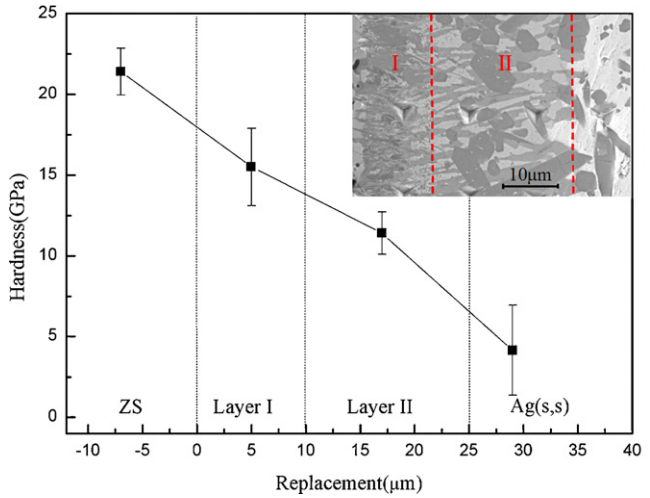

Fig. 3. Average hardness values of various regions in ZS/ZS joint as a function of intender replacement.

results of point 3 show that there is considerable amount of Zr in the gray phase. Based on the atom stoichiometry, the gray phase can be expressed as $AgCu_4Zr$, which is consistent with the "m" phase reported by He et al. in Ref. [14]. The generation of $AgCu_4Zr$ suggests that ZrB_2 had partially dissolved in liquid alloys at brazing temperature. However, in the ZrB_2 grain near the reaction layer (point 5), no penetration was found, indicating the dissolution of ZrB_2 just occurred on the surface of the ZS.

The nanoindentation technique was employed to study the mechanical behaviors of the reaction layer reinforced by TiBw. The tip route started from layer I and ended in Ag(s,s) in the center of the joint, the whole length was 36 μm with an interval displacement of 12 μm. Fig. 3 presents the average hardness values of different areas of the specimen brazed with Ag–Cu/Ti lamination. The average hardness of the ZS substrate is 21.5 GPa, which is slightly lower than the pure ZrB_2 (23 GPa [4]) due to the addition of soft SiC to the ceramic. A gradient reduction in hardness from layer I to Ag(s,s) was observed across the interface. In layer I, Ti–Cu compounds, TiBw and $AgCu_4Zr$ are the main phases. The TiBw array mostly distributed in $AgCu_4Zr$ apparently enhance the hardness of layer I (15.5 GPa) comparing with the layer II (11.4 GPa) which is only comprised of Ti–Cu compound and $AgCu_4Zr$. It is known that joint hardness is sensitive to residual stresses due to CTE mismatch, however, as a discontinuous reinforcement, the dispersive enhancement in hardness by TiBw is not detrimental to joint. In fact, the sufficient TiBw can reasonably match the CTE of the brazing alloy to that of ZS and alleviate the residual thermal stress of the joint, owing to TiBw possess a low CTE of about $8.6 \times 10^{-6}\,K^{-1}$, closely to that of ZS ($7.5 \times 10^{-6}\,K^{-1}$ [15]). The Ag(s,s) in the middle of the joint showed the lowest hardness. As a core of the joint, the Ag(s,s) with excellent ductility and low yield strength can further promote stress accommodation via plastic flow and inhibit cracking tendency thus leading to a sound joint.

3.2. *Effect of Ti content on the interfacial microstructure of ZS/ZS joints*

Fig. 4(a)–(d) shows microstructure of ZS/ZS joints brazed at 900 °C for 10 min with different Ti contents in order to reveal the effect of Ti on the formation of TiBw. In general, the TiB phase is thermodynamically stable with excess Ti. When the filler alloy with 5 wt.% and 10 wt.% Ti was adopted, no obvious TiBw was produced though a part of $AgCu_4Zr$ was formed as shown in Fig. 4(a)–(b). Abundant TiCu and $Ti_5Si_3C_2$ compounds were produced on the interface of ZS. Desired interfacial microstructure was obtained when 15 wt.% Ti was added into filler alloy, as shown in Fig. 4(c). Two gradient layers were formed, which was similar to the joint brazed with Ag–Cu/Ti lamination (Fig. 1(a)). Directional TiBw in the form of clusters grew on the surface of ZrB_2 while the SiC was still covered with Ti–Cu compounds. It should be noted that Ag-based solid solution rather than Ti–Cu or Ti–Si compounds filled in the gap of TiBw to form a Ag/TiBw multiple structure. Since Ag possesses a higher CTE of $20 \times 10^{-6}\,K^{-1}$ while TiB possesses a lower CTE

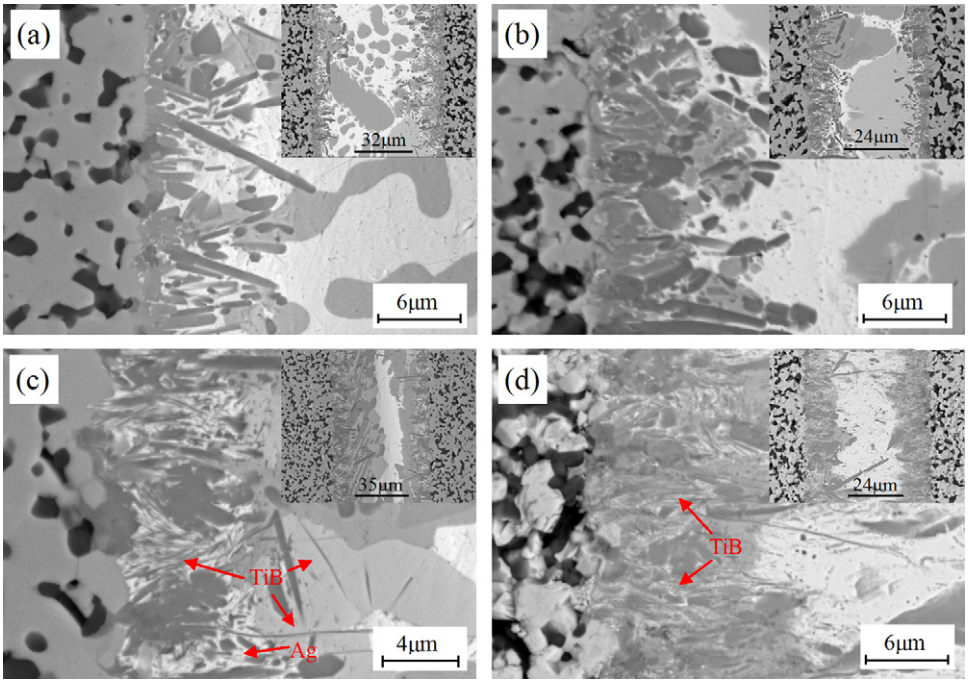

Fig. 4. Backscattered electron micrographs of interfacial microstructure of ZS/ZS joints brazed at 900 °C for 10 min using filler alloy with Ti contents of (a) 5%; (b) 10%; (c) 15%; (d) 20% (wt.%).

of $8.6 \times 10^{-6}\,K^{-1}$, the Ag/TiBw alternate distribution could more effectively relieve the stress caused by CTE mismatch. Additionally, the Ag(s,s) as a ductile material could further absorb stress by plastic deformation, which prevented brittle fracture along the ZS interface. Comparing with Figs. 4(b) and (c), it can be clear that Ti–Cu and Ti–Si series compounds gathered on the interface of the ZS brazed with 15 wt.% Ti was much fewer than the one brazed with 10 wt.% Ti. It is possibly due to the formation of TiBw which inhibited forming Ti–Cu and Ti–Si compounds to some extent by preferentially reacted with Ti around ZS interface. As Ti content increased to 20 wt.% as shown in Fig. 4(d), all Ag was exhausted to form $AgCu_4Zr$ which mainly distributed in the center of the seam. It also can be observed that TiBw on ZS interface has apparently grown up, moreover, complex Ti–Cu–Si and Ti–Si–C compounds were produced accompanied with TiBw on ZS interface.

3.3. Formation mechanism and microstructural evolution of ZS/ZS joints

In order to clarify the joining mechanism, the evolution of interfacial microstructure was preliminary analyzed during brazing process. Since the ZS is composed by two materials (ZrB_2 and SiC) with different stability, the whole reaction process is mainly divided into two stages. Firstly, the less stable SiC ($\Delta G^\circ = -45.3\,kJ\,mol^{-1}$ [16]) reacted with liquid filler alloy to produce a series of Ti–Si–C compounds as shown in Fig. 1(c). It happened at the beginning of brazing and the process was quite fast. After that, if the remaining Ti was adequate, the second stage was launched: the stable ZrB_2 began to dissolve as Ti atoms in liquid alloy diffused to the surface of ZS, reactions can be expressed as below:

$$2(Ti) + \langle ZrB_2\rangle \rightarrow 2\langle TiB\rangle + (Zr) \quad (1)$$

$$(Ti) + \langle ZrB_2\rangle \rightarrow \langle TiB_2\rangle + (Zr) \quad (2)$$

$$(Ti) + \langle TiB_2\rangle \rightarrow 2\langle TiB\rangle \quad (3)$$

The notations $\langle\,\rangle$ and $(\,)$ designate the solid and liquid states, respectively. As the formation Gibbs free energy of TiB_2 is more negative, the dissolution of ZrB_2 was primarily carried out by reaction (2). The equilibrium constant K_c of reaction (2) could be expressed as $K_c = c(Zr)/c(Ti)$. The produced TiB_2 as a transition phase could further react with Ti to form abundant TiBw, as long as the average concentration of B in the reaction zone is less than 18.5 wt.% [17]. Similar reactions have been reported by He et al. [13]. With the dissolution of ZrB_2 progressed by reaction (1) and (2), Zr as production was released and dissolved in Ag(s,s). Combined with Cu in filler alloy, the $AgCu_4Zr$ was produced according to reaction (4):

$$(Ag) + 4(Cu) + (Zr) \rightarrow \langle AgCu_4Zr\rangle \quad (4)$$

Reaction (4) was conducted quickly and thoroughly due to the considerable negative Gibbs free energy ($-340.55\,kJ\,mol^{-1}$ at 900 °C [18]). The consumption of Zr together with sufficient amount of Ti as reactant changed the equilibrium constant K_c and led to the right movement of chemical equilibrium in reaction (2). As a result, the ZrB_2 dissolved slowly and constantly, released B atom to form TiBw. According to previous investigation [19], TiB exhibits much faster growth along the [0 1 0] direction than normal to the (1 0 0), (1 0 1) and (0 0 1) planes, and consequently develops a needle-shaped morphology. In the [0 1 0] direction, Ti atoms and B atoms are in the same stoichiometry, it indicates that TiB preferentially grows along the direction which provides both B atoms and Ti atoms sufficiently. Therefore, the orientation of TiB is vertical to interface and consistent with the diffusion direction.

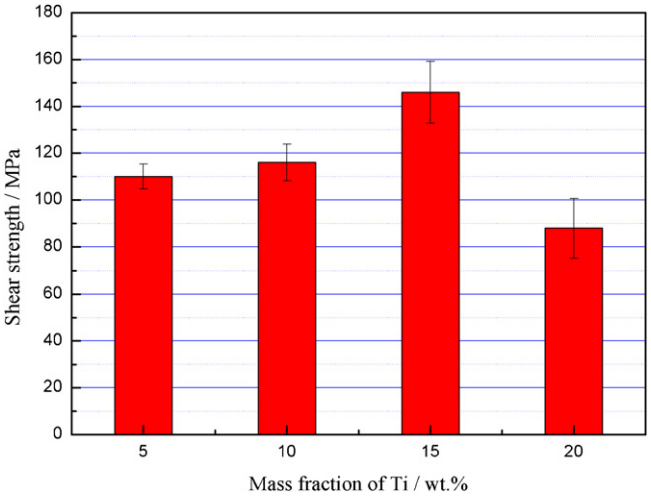

Fig. 5. Effect of Ti content on shear strength of brazed joints.

3.4. Mechanical properties of ZS/ZS joints

Fig. 5 illustrates the shear strengths of ZS/ZS joints using filler alloys with different Ti contents at 900 °C for 10 min. The maximum shear strength of 146 MPa was attained when the content of Ti was 15 wt.%. As seen from Fig. 5, when the mass fraction of Ti was 5 wt.% and 10 wt.%, the shear strength had nearly no change. The experimental results can be explained as following. When Ti content of filler alloys was relatively low, abundant Ag(s,s) was produced and distributed in nearly whole seam (Fig. 4(a)). High stress concentration and residual stresses are induced near the interface between ZS and filler alloy due to the large difference in elastic modulus and thermal expansion coefficient of ceramics and metals. The fracture of test samples usually occurred in ZS substrate near the seam. As Ti content increased to 10 wt.%, various Ti–Cu and Ti–Si compounds were produced along the ZS interface, which was detrimental to the joint strength. Desired interfacial microstructure was obtained when Ti content was 15 wt.%. Mechanics performance improvements stemmed from the TiBw/Ag alternative structure which accommodated residual stresses on ZS interface, additionally, gradient layers from ZS to the center of the joint, which was similar to the sample brazed with AgCu/Ti lamination (as shown in Fig. 1(a)), was fabricated and resulted in the release of the residual stress and increase of the joining quality. The test samples with 15 wt.% Ti usually cracked along Ag-based solid solution in the middle of the seam and demonstrated a ductile fracture as shown in Fig. 6. With further increasing Ti content to 20 wt.%, the shear strength decreased sharply due to abundant brittle compounds produced on the ZS interface. Excess Ti caused severely dissolving of ZrB_2 and SiC during brazing, which not only degraded the properties of ZS, but also increase brittleness of the joint.

The fracture morphology of sample brazed with 15 wt.% Ti content was investigated as shown in Fig. 6. Based on the EDS results, cracks propagated mainly through layer II, Ag(s,s) and ZS substrate. Some low-lying areas (Fig. 6(b)) going deep into layer I were observed on the rugged fracture surface of layer II. There are a large number of TiBw lie in the edge of cleavage fracture, indicating the cracks have been deflected as they propagated to the axis of TiB. The extensive crack deflection and TiB pullout undoubtedly led to the increase in fracture toughness. As cracks propagated toward the center of joint, they shifted to the interior of the brazed area far from the interfacial layer on the joint. According to the EDS analysis, the fracture region which occupies most fracture surface of the joint is Ag(s,s) and Ag–Cu eutectic. The fractograph (Fig. 6(c)) demonstrates ductile fracture with sliding marks due to the existence

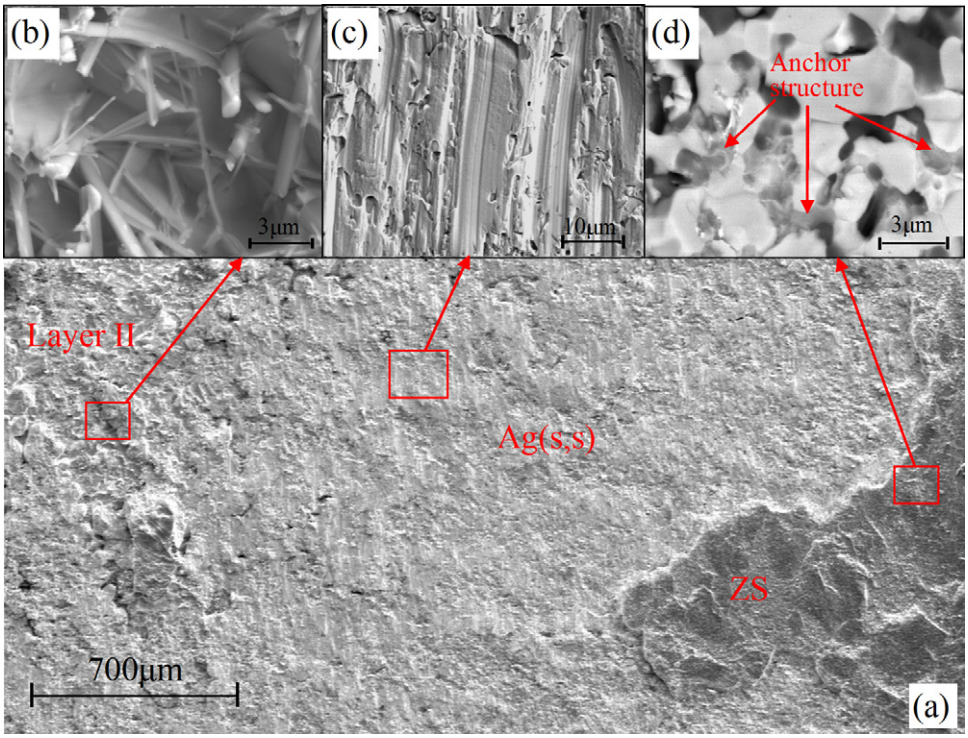

Fig. 6. Typical fractural surfaces of ZS/ZS joint brazed with the Ag–Cu/Ti filler alloy containing 15 wt.% Ti at 900 °C for 10 min: (a) fracture of ZS/ZS joint; (b), (c) and (d) magnifications of the marked areas in (a).

of inherently ductile Ag, which is favorable for the strength of the joint. Additionally, a part of thin ZS layer was also observed on the fractograph, the magnified image (Fig. 6(d)) indicates that the "anchor structure", which further improves interfacial adhesion, is the main reason for causing fracture propagation on ZS substrate.

4. Conclusions

In summary, the ZS/ZS was successfully joined with Ag–Cu/Ti filler alloy by brazing. A novel TiBw array with high orientation along the interface of ZS was in situ synthesized during brazing for the first time. The precipitation of $AgCu_4Zr$ and sufficient content of Ti played a key role in formation of TiBw. The TiBw serving as an adjusting phase effectively relieved the CTE mismatch and finally resulted in an intimate integrity. Additionally, the "anchor structure" due to severe reaction between SiC and liquid alloy further improved the joining strength. The highest shear strength of 146 MPa was reached by the joints brazed with the filler alloy containing 15 wt.% Ti.

Acknowledgments

The authors gratefully acknowledge the financial support from the Fundamental Research Funds for the Central Universities (grant nos. HIT.BRET1.2010006, HIT.NSRIF.2010119 and HIT.NSRIF.201135), National Natural Science Foundation of China (NSFC, grant nos. 50975062, 51105107 and 51021002), Specialized Research Fund for the Doctoral Program of Higher Education (grant no. 20112302130005), Natural Science Foundation of Heilongjiang Province (grant no. QC2011C044) and the China Postdoctoral Science Foundation funded project (CPSF, grant no. 20100471027).

References

[1] S.Q. Guo, J. Eur. Ceram. Soc. 29 (2009) 995–1011.
[2] H.M. Chen, F. Zheng, H.S. Liu, L.B. Liu, Z.P. Jin, J. Alloys Compd. 468 (2009) 209–216.
[3] K. Upadhya, J.M. Yang, W.P. Hoffman, Am. Ceram. Soc. Bull. 76 (1997) 51–56.
[4] W.G. Fahrenholtz, G.E. Hilmas, I.G. Talmy, J.A. Zaykoski, J. Am. Ceram. Soc. 90 (2007) 1347–1364.
[5] Z. Wang, S. Wang, X.H. Zhang, P. Hu, W.B. Han, C.Q. Hong, J. Alloys Compd. 484 (2009) 390–394.
[6] J.H. Xiong, J.H. Huang, H. Zhang, X.K. Zhao, Mater. Sci. Eng. A 527 (2010) 1096–1101.
[7] M. Galli, J. Cugnoni, J. Botsis, J. Janczak-Rusch, Compos. Part A 39 (2008) 972–978.
[8] J. Xiong, J. Huang, Z. Wang, G. Lin, H. Zhang, X. Zhao, Mater. Sci. Technol. 25 (2009) 1046–1050.
[9] G. Blugan, J. Kuebler, V. Bissig, J. Janczak-Rusch, Ceram. Int. 33 (2007) 1033–1039.
[10] J.G. Yang, H.Y. Fang, X. Wan, J. Mater. Sci. Technol. 21 (2005) 782–784.
[11] G.B. Lin, J.H. Huang, Powder Metall. 49 (2006) 345–348.
[12] M.X. Yang, T.S. Lin, P. He, Mater. Sci. Eng. A 528 (2011) 3520–3525.
[13] P. He, M.X. Yang, T.S. Lin, Z. Jiao, J. Alloys Compd. 509 (2011) 289–292.
[14] X.C. He, Y.M. Wang, H.S. Liu, Z.P. Jin, J. Alloys Compd. 439 (2007) 176–180.
[15] M. Singh, R. Asthana, J. Mater. Sci. 45 (2010) 4308–4320.
[16] Y. Liu, Z.R. Huang, X.J. Liu, Ceram. Int. 35 (2009) 3479–3484.
[17] K.B. Panda, K.S.R. Chandran, Metall. Mater. Trans. A 34 (2003) 1371–1385.
[18] D.H. Kang, I.H. Jung, Intermetallics 18 (2010) 815–833.
[19] H.B. Feng, Y. Zhou, D.C. Jia, Q.C. Meng, Scripta Mater. 55 (2006) 667–670.